

DOS: Directional Object Separation in Text Embeddings for Multi-Object Image Generation

Dongnam Byun^{1,3}, Jungwon Park¹, Jungmin Ko², Changin Choi^{2,4}, Wonjong Rhee^{1,2}

¹Department of Intelligence and Information, Seoul National University

²Interdisciplinary Program in Artificial Intelligence, Seoul National University

³Samsung Research, Samsung Electronics

⁴SAIT, Samsung Electronics

{east928, quoded97, jungminko, ci2015.choi, wrhee}@snu.ac.kr

Abstract

Recent progress in text-to-image (T2I) generative models has led to significant improvements in generating high-quality images aligned with text prompts. However, these models still struggle with prompts involving multiple objects, often resulting in *object neglect* or *object mixing*. Through extensive studies, we identify four problematic scenarios, Similar Shapes, Similar Textures, Dissimilar Background Biases, and Many Objects, where inter-object relationships frequently lead to such failures. Motivated by two key observations about CLIP embeddings, we propose DOS (Directional Object Separation), a method that modifies three types of CLIP text embeddings before passing them into text-to-image models. Experimental results show that DOS consistently improves the success rate of multi-object image generation and reduces object mixing. In human evaluations, DOS significantly outperforms four competing methods, receiving 26.24%-43.04% more votes across four benchmarks. These results highlight DOS as a practical and effective solution for improving multi-object image generation.

Code — <https://github.com/dongnami/DOS>

1 Introduction

Recent progress in text-to-image (T2I) generative models has led to substantial improvements in generating high-quality images that closely align with text prompts (Podell et al. 2023; Stability AI 2024; Black Forest Labs 2025). These models leverage text embeddings from multiple CLIP (Radford et al. 2021) encoders, and optionally the T5 (Raffel et al. 2020) encoder, to enhance image-text alignment. However, they still struggle to accurately generate images containing multiple objects. In this work, we identify four scenarios where this issue becomes particularly severe and demonstrate that modifying the CLIP text embeddings, without altering the image generation process within the text-to-image models, can substantially mitigate the problem.

Previous work on multi-object image generation has primarily focused on the relationships between nouns and their associated attributes (Rassin et al. 2023; Zhuang, Hu, and Gao 2024; Hu et al. 2024a), often overlooking challenges

that arise from interactions between multiple noun entities. However, through extensive experiments with state-of-the-art T2I models, we find that failures, specifically *object neglect* or *object mixing*, occur frequently in scenarios involving inter-object relationships, even when no attributes are present. To investigate these issues more thoroughly, we focus on prompts that primarily contain objects and avoid descriptive attributes. Following extensive exploration and experimentation, we identify four types of problematic scenarios. As shown in Figure 1, the first three categories represent specific types of inter-object relationships where failures become particularly severe: *Similar Shapes*, *Similar Textures*, and *Dissimilar Background Biases*. *Background bias* refers to the natural background typically associated with each object (e.g., ‘land’ for ‘deer’ vs. ‘sea’ for ‘sea turtle’). The fourth, *Many Objects*, captures the compounded effect of numerous inter-object relationships, which may include but are not limited to the first three types.

The motivation for our method stems from two previously reported observations regarding CLIP text embeddings used in T2I models: (1) CLIP employs a causal masking mechanism, where information from earlier tokens is mixed into later token embeddings, leading to *information mix-ups* in the embeddings of later tokens (Zhuang, Hu, and Gao 2024; Chen et al. 2024), (2) the difference between two CLIP text embeddings appears to encode directional information, which can be indirectly observed through the behavior of T2I models (Hu et al. 2024a). Our method aims to mitigate information mix-ups in CLIP text embeddings by constructing directional vectors, referred to as *separation vectors*, derived from the difference between two CLIP embeddings. These vectors are added to the original text embeddings to inject directional information that encourages the separation of object-specific information.

Our method, called DOS (Directional Object Separation), constructs a separation vector for each object pair and each type of CLIP text embedding, namely semantic token embeddings of all object nouns, EOT embeddings, and pooled embeddings, to encode directional information that promotes separation. For each embedding type, the separation vectors of all object pairs are combined through a weighted average, where the weights reflect the difficulty of separating each corresponding pair. This weighted combination forms the DOS vector, which is then added to the original text em-

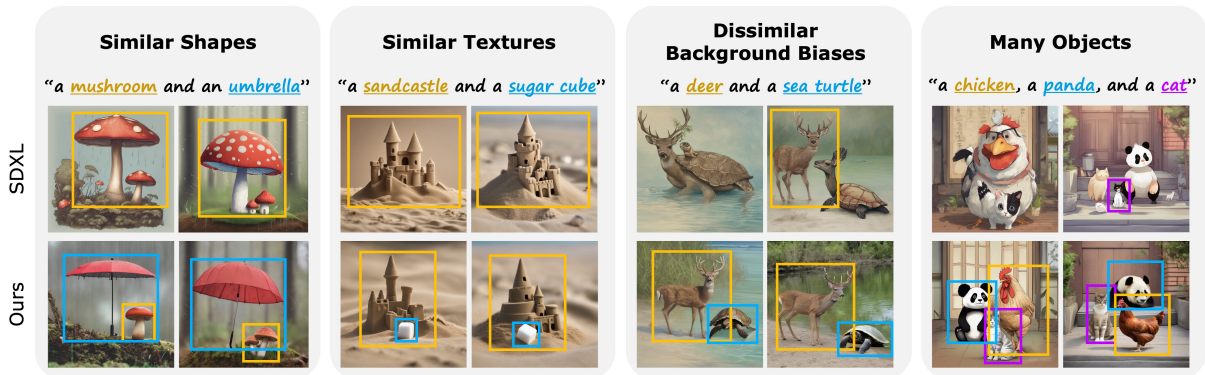


Figure 1: Text-to-image generative models often struggle to generate images with multiple objects, especially in four scenarios where relationships between objects, referred to as *inter-object relationships*, frequently lead to object neglect or object mixing: Similar Shapes, Similar Textures, Dissimilar Background Biases, and Many Objects. Our method mitigates these failures by modifying text embeddings before feeding them into the text-to-image model.

beddings.

Across four benchmarks corresponding to the problematic scenarios of *Similar Shapes*, *Similar Textures*, *Dissimilar Background Biases*, and *Many Objects*, DOS improves the success rate of multi-object image generation while reducing object mixing. In human evaluations, compared to four other models including the baseline, DOS received 26.24%-43.04% more votes than the second-best results across the four benchmarks. Since DOS does not alter the image generation process within the text-to-image model, its inference is approximately four times faster than well-known latent modification methods such as Attend-and-Excite (Chefer et al. 2023). These results demonstrate that DOS is both an effective and efficient algorithm for addressing object neglect and object mixing, which frequently arise from inter-object relationships in multi-object image generation.

2 Related Work

Multi-object image generation involves generating images containing multiple objects, optionally along with their associated attributes. However, during generation, interactions among multiple objects, and optionally their associated attributes, often lead to failures such as object neglect, object mixing, or inaccurate attribute binding. A substantial body of work has been proposed to address these issues (Chefer et al. 2023; Hu et al. 2024b; Jiang et al. 2024). Among them, Attend-and-Excite (Chefer et al. 2023) demonstrates that iteratively updating the intermediate image latent can reduce such failures. This inspired a series of follow-up methods based on latent modification, such as CONFORM (Meral et al. 2024). While effective to some extent, these methods typically require expensive iterative gradient updates during inference and often introduce visual artifacts due to deviations from the latent distribution the model was trained on. To overcome these limitations, more recent approaches have focused on modifying only the text embeddings—without altering the intermediate image latent (Chen et al. 2024; Hu et al. 2024a; Zhuang, Hu, and Gao 2024). Among these, TEBOpt (Chen et al. 2024) proposes modifying the semantic token embeddings corresponding to each object to bet-

ter separate them. This approach significantly reduces information bias (i.e., cases where certain objects are more frequently generated than others), but shows only limited improvements in addressing object neglect and object mixing. In contrast, our method leverages *directional information* to modify all types of CLIP text embeddings—not only semantic token embeddings, but also EOT and pooled embeddings—in a way that promotes object separation, significantly reducing both object neglect and object mixing in multi-object image generation.

3 Preliminary Analysis

In Figure 1, we identify four types of problematic scenarios involving inter-object relationships: *Similar Shapes*, *Similar Textures*, *Dissimilar Background Biases*, and *Many Objects*. To examine how each of these scenarios intensifies object neglect or object mixing, we analyze four corresponding aspects in multi-object image generation. For each aspect, we construct two sets of multi-object prompts that contrast in condition. For example, under the shape aspect, the *dissimilar shapes* condition consists of 20 prompts featuring two objects with dissimilar shapes, following the template “a/an {object A} and a/an {object B}.” In contrast, the *similar shapes* condition includes 20 prompts with two similarly shaped objects. The conditions for the other three aspects are defined analogously. Full details on the construction of all prompt sets are provided in Table 6 of Appendix A.

We generate images for each prompt using 10 random seeds, resulting in 200 images per condition. We then compute the success rate, defined as the percentage of images that exhibit neither object neglect nor object mixing. Figure 2 presents both the quantitative results (top row) and a qualitative example (bottom row) for each condition across the four aspects. The observed differences in success rates between the two contrasting conditions range from 26.5% to 60.5%. These findings demonstrate that the four identified scenarios significantly intensify generation failures and motivate our focus on addressing them to reduce object neglect and mixing in multi-object image generation.

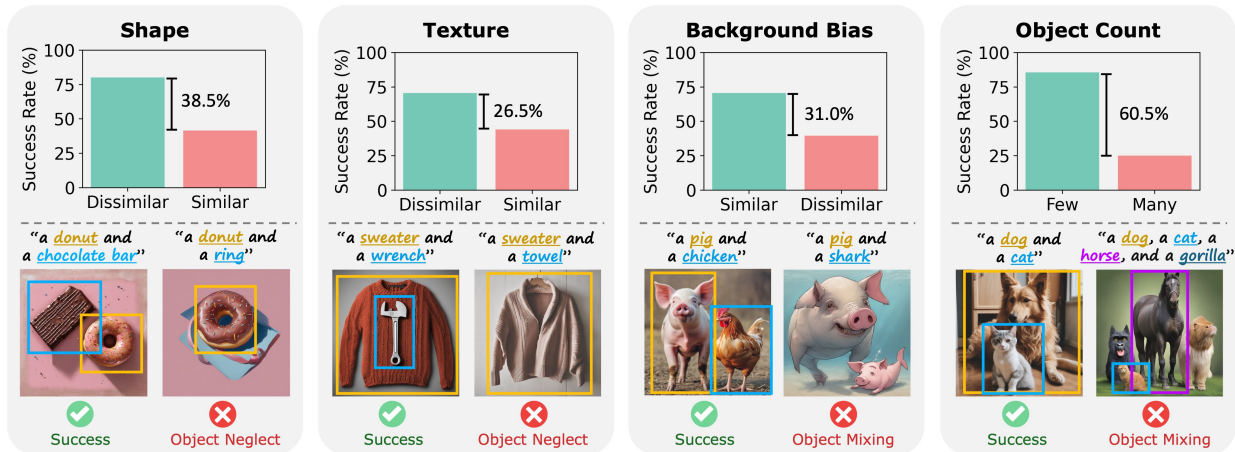


Figure 2: Analysis of four aspects of inter-object relationships in multi-object image generation. The top row shows quantitative comparisons between two contrasting conditions for each aspect, while the bottom row shows a qualitative example for each condition. A lower success rate indicates more frequent failures, such as object neglect or object mixing.

4 DOS: Directional Object Separation in Text Embeddings

Background on CLIP text embeddings in text-to-image generative models. Let P be the input prompt for image generation, which is passed through CLIP text encoders to produce the CLIP text embedding: $[c_{\text{SOT}}, c_{t_1}, \dots, c_{t_L}, c_{\text{EOT}}, c_{\text{PAD}}, \dots, c_{\text{PAD}}] \in \mathbb{R}^{77 \times d}$, where SOT, EOT, and PAD denote special tokens indicating the start-of-text, end-of-text, and padding respectively; t_i denotes the i -th semantic token; and d is the embedding dimension. Recent T2I models such as SDXL also use a pooled embedding c_{pool} , which is computed by applying a linear projection to the end-of-text (EOT) embedding c_{EOT} . All these text embeddings are then used to condition the T2I model during image generation. Our method modifies these embeddings before passing them to the T2I model to mitigate object neglect and object mixing in multi-object image generation.

Overview of the proposed method. Suppose the input text prompt P contains N object nouns, where the n -th object noun is denoted by obj_n for all $n \in \{1, 2, \dots, N\}$. Let c_{obj}^n denote the semantic token embedding corresponding to obj_n . Additionally, let c_{EOT} and c_{pool} denote the EOT and pooled embeddings, respectively. Our method modifies all of these CLIP text embeddings by adding DOS vectors to each embedding. These DOS vectors are computed by aggregating separation vectors across all object pairs, where each separation vector defines a direction that distinguishes one object from the other in the pair. The following subsections describe: (1) how the separation vectors are computed for each object pair, (2) how the strength of each separation vector is adjusted prior to aggregation, and (3) how the adjusted vectors are combined to construct the final DOS vectors for each type of embedding. An overview of our method is illustrated in Figure 3.

Computing pairwise separation vectors. The separation vectors for each object pair (obj_n, obj_m) are designed to en-

code directional information that promotes separation from obj_m to obj_n . These vectors are computed differently depending on the type of text embedding. For the semantic token embedding c_{obj}^n , the separation vector is defined as the difference between two object-specific embeddings, $c_{obj}^{\text{pure},n}$ and $c_{obj}^{\text{pure},m}$, each obtained from a pure prompt of the form $P_{\text{pure},i} = \text{“a } \{obj_i\}\text{”}$ for $i = n, m$, respectively:

$$s_{obj}^{(n,m)} = c_{obj}^{\text{pure},n} - c_{obj}^{\text{pure},m} \quad (1)$$

Using pure prompts ensures that $c_{obj}^{\text{pure},n}$ and $c_{obj}^{\text{pure},m}$ capture clean, object-specific representations by avoiding undesirable information mix-ups across tokens. In contrast, for EOT and pooled embeddings, we intentionally exploit information mix-ups to define separation vectors. Specifically, we construct two contrastive prompts: $P_{\text{sep},(n,m)} = \text{“a } \{obj_n\} \text{ separated from a } \{obj_m\}\text{”}$ and $P_{\text{mix},(n,m)} = \text{“a } \{obj_n\} \text{ mixed with a } \{obj_m\}\text{”}$. From these, we extract the corresponding EOT and pooled embeddings, denoted as $c_{\text{EOT/pool}}^{\text{sep},(n,m)}$ and $c_{\text{EOT/pool}}^{\text{mix},(n,m)}$, and define the separation vectors as:

$$s_{\text{EOT/pool}}^{(n,m)} = c_{\text{EOT/pool}}^{\text{sep},(n,m)} - c_{\text{EOT/pool}}^{\text{mix},(n,m)} \quad (2)$$

While we use the unified notation $s_{\text{EOT/pool}}^{(n,m)}$ for brevity, these separation vectors are computed independently for the EOT and pooled embeddings. Overall, our separation vector design extracts directional signals that promote object separation: by avoiding information mix-ups for semantic token embeddings, and by deliberately exploiting contrastive prompts to leverage such mix-ups for EOT and pooled embeddings.

Computing pairwise adaptive strengths. In Figure 2, we observed that certain object pairs are more susceptible to object neglect or object mixing than others. Motivated by this observation, we adjust the strength of the separation vectors for each object pair based on their visual (shape and texture) similarities and background bias dissimilarities. To

this end, we first select 42 representative words covering a diverse range of object shapes and textures through interactions with GPT-o4-mini-high (OpenAI 2025) and define prompts of the form $P_{\text{attr},(k,n)} = \text{“a } \{attribute_k\} \{obj_n\}\text{”}$ for all $k \in \{1, 2, \dots, 42\}$. Similarly, we select 36 representative background phrases and define prompts of the form $P_{\text{bg},(l,n)} = \text{“}\{background_l\}, \text{there is a } \{obj_n\}\text{”}$ for all $l \in \{1, 2, \dots, 36\}$. We then compare the text embeddings $\mathbf{c}_{\text{obj}/\text{EOT}/\text{pool}}^{\text{pure},n}$ obtained from the pure prompt $P_{\text{pure},n} = \text{“a } \{obj_n\}\text{”}$, with embeddings $\mathbf{c}_{\text{obj}/\text{EOT}/\text{pool}}^{\text{attr},(k,n)}$ and $\mathbf{c}_{\text{obj}/\text{EOT}/\text{pool}}^{\text{bg},(l,n)}$ obtained from the attribute and background prompts, respectively. Cosine similarity is used for this comparison:

$$\mathbf{a}_\tau^{\text{attr},n}[k] = \text{sim}(\mathbf{c}_\tau^{\text{pure},n}, \mathbf{c}_\tau^{\text{attr},(k,n)}), \quad (3)$$

$$\mathbf{a}_\tau^{\text{bg},n}[l] = \text{sim}(\mathbf{c}_\tau^{\text{pure},n}, \mathbf{c}_\tau^{\text{bg},(l,n)}), \quad (4)$$

for $k \in \{1, 2, \dots, 42\}$, $l \in \{\text{obj}, \text{EOT}, \text{pool}\}$, and $\tau \in \{\text{obj}, \text{EOT}, \text{pool}\}$, where τ denotes the type of text embedding. The resulting lists of cosine similarities $\mathbf{a}_\tau^{\text{attr},n}$ and $\mathbf{a}_\tau^{\text{bg},n}$ reflect how closely obj_n aligns with the predefined visual attributes and background contexts. We compute the same lists for obj_m , and define the adaptive strength for the object pair (obj_n, obj_m) as:

$$\alpha_\tau^{(n,m)} = \max \left\{ \sigma(\rho(\mathbf{a}_\tau^{\text{attr},n}, \mathbf{a}_\tau^{\text{attr},m}); x_{\tau,0}^{\text{attr}}), \sigma(1 - \rho(\mathbf{a}_\tau^{\text{bg},n}, \mathbf{a}_\tau^{\text{bg},m}); x_{\tau,0}^{\text{bg}}) \right\}, \quad (5)$$

for $\tau \in \{\text{obj}, \text{EOT}, \text{pool}\}$, where $\rho(\cdot, \cdot)$ denotes Pearson correlation, which is used to avoid mean and scaling effects, and $\sigma(x; x_{\tau,0})$ is a shifted tempered sigmoid function defined as:

$$\rho(x, y) = \frac{\sum_t (x_t - \bar{x})(y_t - \bar{y})}{\sqrt{\sum_t (x_t - \bar{x})^2} \sqrt{\sum_t (y_t - \bar{y})^2}}, \quad (6)$$

$$\sigma(x; x_{\tau,0}) = (1 + \exp\{-(x - x_{\tau,0})/T\})^{-1} \quad (7)$$

Here, the offset $x_{\tau,0}^{\text{attr}}$ is the mean of $\rho(\mathbf{a}_\tau^{\text{attr},i}, \mathbf{a}_\tau^{\text{attr},j})$ over all object pairs (obj_i, obj_j) from the MS-COCO (Lin et al. 2014) dataset. Similarly, $x_{\tau,0}^{\text{bg}}$ is the mean of $(1 - \rho(\mathbf{a}_\tau^{\text{bg},i}, \mathbf{a}_\tau^{\text{bg},j}))$ over the same object pairs. These adaptive strengths promote stronger separation for object pairs that are more likely to be mixed or neglected, thereby helping to reduce object neglect and mixing in multi-object image generation. In Appendix B.1, we provide the full list of 42 representative words describing object shapes and textures and 36 representative background phrases, which are used to construct the prompts $P_{\text{attr},(k,n)}$ and $P_{\text{bg},(l,n)}$, respectively.

Updating text embeddings. Finally, the DOS vectors for the semantic token, EOT, and pooled embeddings are computed as a weighted average of the separation vectors, where each weight corresponds to the adaptive strength of a given object pair:

$$\mathbf{v}_\tau^{\text{DOS},n} = \frac{1}{N-1} \sum_{m \neq n} \alpha_\tau^{(n,m)} \mathbf{s}_\tau^{(n,m)}, \quad (8)$$

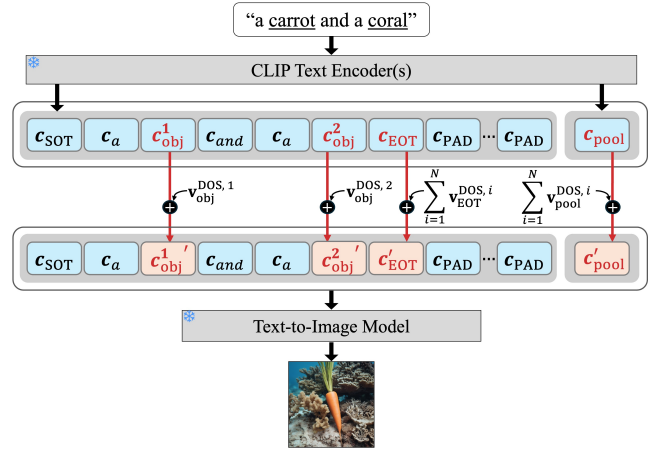


Figure 3: Method Overview. DOS vectors are computed for the semantic token embeddings corresponding to object nouns, the EOT embedding, and the pooled embedding. These vectors are added to the corresponding CLIP text embeddings, namely $\mathbf{c}_{\text{obj}}^n$ for $n = 1, \dots, N$, \mathbf{c}_{EOT} , and \mathbf{c}_{pool} , before being passed into the text-to-image model. N denotes the number of object nouns in the prompt.

where $\tau \in \{\text{obj}, \text{EOT}, \text{pool}\}$, and $n \in \{1, 2, \dots, N\}$. These DOS vectors are then added to the original text embeddings, which are subsequently passed into the T2I model. Specifically, semantic token embeddings corresponding to object nouns are updated as:

$$\mathbf{c}_{\text{obj}}^n' = \mathbf{c}_{\text{obj}}^n + \mathbf{v}_{\text{obj}}^{\text{DOS},n}, \quad (9)$$

for $n \in \{1, 2, \dots, N\}$. If obj_n consists of multiple tokens, their semantic token embeddings are first averaged before computing the DOS vector, and the resulting DOS vector is then added to each of the semantic token embeddings that constitute obj_n . In addition, the EOT and pooled embeddings are updated by summing the DOS vectors across all objects:

$$\mathbf{c}'_{\text{EOT}/\text{pool}} = \mathbf{c}_{\text{EOT}/\text{pool}} + \sum_{i=1}^N \mathbf{v}_{\text{EOT}/\text{pool}}^{\text{DOS},i} \quad (10)$$

While we use the unified notation $\mathbf{c}_{\text{EOT}/\text{pool}}$ and $\mathbf{c}'_{\text{EOT}/\text{pool}}$ for brevity, the EOT and pooled embeddings are computed and updated independently. This aggregation across all objects is intended to mitigate the compounded effects of inter-object relationships in multi-object image generation.

5 Experiments

5.1 Experimental Setup

Implementation details. Our method is based on SDXL (Podell et al. 2023) and has also been implemented on the recently released Stable Diffusion 3.5 (SD3.5) (Stability AI 2024). We apply DOS updates to all CLIP text embeddings used by each model. For inference, we use a guidance scale of 5.0 with 50 denoising steps for SDXL, and a guidance scale of 7.0 with 28 steps for SD3.5, which are the official default configurations. The temperature T

Base Model	Method	Similar Shapes		Similar Textures		Dissimilar Background Biases		Many Objects	
		SR↑	MR↓	SR↑	MR↓	SR↑	MR↓	SR↑	MR↓
SDXL	Base	48.00%	6.50%	58.00%	7.50%	46.00%	22.50%	23.00%	27.50%
	TEBOpt	52.00%	5.00%	61.00%	4.00%	44.50%	23.00%	24.00%	27.00%
	A&E	60.50%	6.00%	67.50%	5.00%	53.50%	25.00%	28.50%	28.50%
	CONFORM	54.00%	6.50%	64.50%	9.00%	55.50%	22.00%	37.50%	26.50%
	Ours	64.00%	3.50%	71.50%	3.50%	68.50%	17.00%	48.00%	15.50%
SD3.5	Base	75.50%	4.00%	79.00%	6.00%	78.00%	17.50%	70.00%	16.50%
	Ours	81.00%	3.00%	87.50%	3.00%	85.50%	13.50%	76.50%	10.50%

Table 1: Quantitative comparison across four benchmarks: Similar Shapes, Similar Textures, Dissimilar Background Biases, and Many Objects. SR denotes Success Rate (↑ higher is better), and MR denotes Mixture Rate (↓ lower is better).

Method	Similar Shapes	Similar Textures	Dissimilar Background Biases	Many Objects
SDXL	7.59%	9.38%	3.59%	3.21%
TEBOpt	7.24%	7.03%	4.22%	4.82%
A&E	13.62%	14.84%	22.81%	11.43%
CONFORM	12.76%	16.88%	12.19%	12.14%
Ours	50.52%	43.12%	53.44%	55.18%
No winner	8.28%	8.75%	3.75%	13.21%

Table 2: Results of human preference studies across four benchmarks. All methods are based on SDXL.

	SDXL	TEBOpt	A&E	CONFORM	Ours
Inference Time (s)	12.97	13.50	58.83	58.48	13.87

Table 3: Inference time comparison (in seconds). All values are averaged over 10 runs. All methods are based on SDXL.

of the shifted tempered sigmoid functions in Eq. 7 is set to $T = 0.6$ for all base models, determined through a light validation process. Additional implementation details are provided in Appendix B.1.

Dataset. To focus on the four problematic scenarios in multi-object image generation, we construct four corresponding benchmarks: Similar Shapes, Similar Textures, Dissimilar Background Biases, and Many Objects. Each of the first three benchmarks consists of 50 two-object prompts, following the template: “a/an {object A} and a/an {object B}.” The object pairs for these benchmarks are selected through interactions with GPT-o4-mini-high (OpenAI 2025). For the Many Objects benchmark, we extend the animal list used in Attend-and-Excite to include 17 animals, from which we randomly sample to create 25 three-object prompts and 25 four-object prompts. For each method, we generate 4 images per prompt using different random seeds, resulting in 200 generated images per benchmark. While the main experiment for Many Objects focuses on the animal list, we present results for an extended benchmark in Table 11 of Appendix C.3 that also includes electronics, vehicles, and fruits. Detailed information about the construction of each benchmark is provided in Appendix B.2.

Evaluation metrics. We adjust the VLM-based metric from EnMMDiT (Wei et al. 2024) to measure both the suc-

cess rate (SR) and mixture rate (MR) for each generated image. SR evaluates whether all the objects specified in the prompt are clearly present in the image, while MR assesses whether any of the objects appear mixed. Specifically, we provided GPT-4o-mini with the generated image and the text prompt used for image generation, asking it to classify each object in the prompt as (1) fully intact, (2) mixed, or (3) absent. SR is calculated as the ratio of images where all objects are classified as fully intact, and MR is calculated as the ratio of images where one or more objects are classified as mixed. A high SR score and a low MR score indicate superior image-text alignment. We further validate the consistency of the results across two additional evaluators in Table 13 of Appendix C.6. Additional details about the VLM-based metrics are provided in Appendix B.3.

5.2 Experimental Results

We compare our method with TEBOpt (Chen et al. 2024), Attend-and-Excite (A&E) (Chefer et al. 2023), and CONFORM (Meral et al. 2024) using SDXL as the base model. For SD3.5, we only compare our method with the baseline model in our main experiment. Further comparisons on SD3.5 against recent methods, TEBOpt (Chen et al. 2024) and Self-Cross (Qiu, Wang, and Tang 2025), are provided in Table 14 of Appendix C.7.

Qualitative comparison. Qualitative comparisons for each problematic scenario are shown in Figure 4. Across all scenarios and base models, our method successfully generates all objects specified in the prompts, while other methods often exhibit object neglect or object mixing. For example, given the prompt “a carrot and an ice cream cone,” our method successfully generates both objects without mixing, whereas the other methods fail to do so. In Figure 5, we also compare results on more complex prompts, where our method continues to show better generations. Additional qualitative results, including examples with complex prompts, are provided in Figures 12-17 of Appendix C.8.

Quantitative comparison. Table 1 presents quantitative comparisons across all four benchmarks in multi-object image generation. Across all benchmarks and base models, our method achieves the highest success rate (SR) (higher is better) and the lowest mixture rate (MR) (lower is better). Specifically, our method outperforms TEBOpt, which is the other text embedding modification method, by 10.50%-

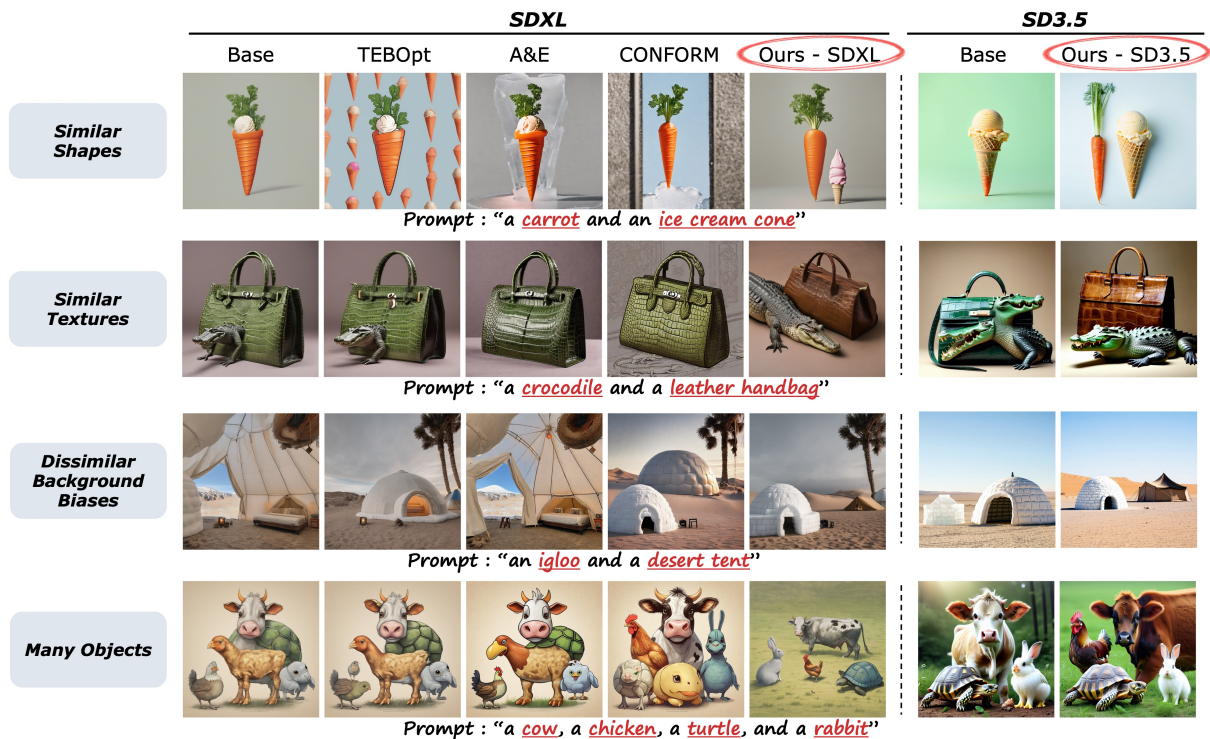


Figure 4: Qualitative comparison across four benchmarks: *Similar Shapes*, *Similar Textures*, *Dissimilar Background Biases*, and *Many Objects*. More results are shown in Figures 14-16 of Appendix C.8.

24.00% in SR. It also surpasses the latent modification methods A&E and CONFORM, which generally require much higher inference time compared to ours. On the recently released SD3.5 model, our method further improves over the baseline, demonstrating that its effectiveness extends to newer architectures.

Human preference study. We conducted human preference studies across all four benchmarks in multi-object image generation. In each survey, participants were presented with five images generated from the same text prompt but using different SDXL-based methods, and asked to select the one that best represents all the objects specified in the prompt. Participants were instructed to avoid images with object neglect or object mixing. Using Amazon Mechanical Turk (MTurk), we collected 580, 640, 640, 560 responses from 29, 32, 32, 28 valid participants for each survey, respectively. As shown in Table 2, our method significantly outperforms the others, receiving 26.24%-43.04% more votes than the second-best results across the four benchmarks. Additional details on the human preference studies, including survey questions and participant filtering criteria, are provided in Appendix B.4.

5.3 Analysis

Inference time comparison. To demonstrate the time efficiency of our method, we compare the inference times of various SDXL-based methods. As shown in Table 3, text embedding modification methods, including TEBOpt and our method, exhibit inference times similar to the baseline

model, indicating minimal time overhead for modifying text embeddings. In contrast, latent modification methods A&E and CONFORM require approximately 4-5 times more computational time than the baseline, due to the iterative gradient updates during image generation. This highlights that our method offers both an efficient and effective solution to the challenges of multi-object generation.

Ablation on text embedding types. Our method applies DOS updates to three types of CLIP text embeddings: semantic token embeddings corresponding to object nouns, EOT embeddings, and pooled embeddings. In Table 4, we ablate the type of embeddings to which DOS is applied. The results show that applying DOS to either the semantic token embeddings or the EOT/pooled embeddings leads to notable improvements in SR, while MR is more significantly reduced when DOS is applied to EOT/pooled embeddings. This is likely because EOT and pooled embeddings tend to capture the overall semantics of the prompt (Wu, Yang, and Wang 2024), influencing the overall spatial structure of the generated images when modified. Finally, applying DOS to all three types of embeddings results in the best performance on both SR and MR. Qualitative examples for this ablation study are shown in Figure 10 of Appendix C.2.

Ablation on adaptive strengths. To examine the effect of the adaptive strengths defined in Eq. 5, we perform an ablation by setting all adaptive strengths to a fixed value of 0.5. The results, shown in Table 5, indicate that using the fixed strength for all separation vectors already leads to substan-

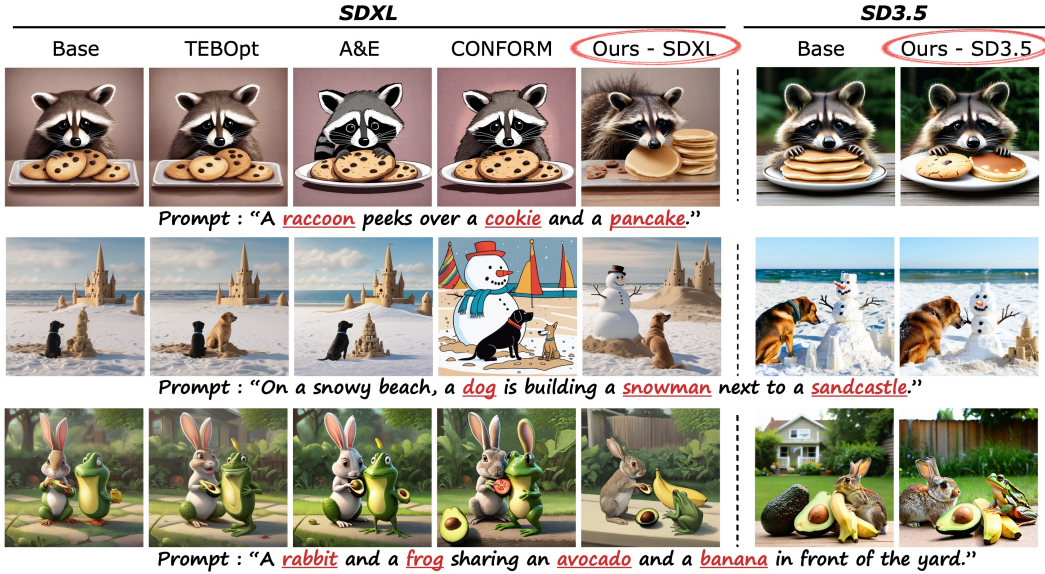


Figure 5: Qualitative comparison on complex prompts. More results are shown in Figure 17 of Appendix C.8.

Method	Similar Shapes		Similar Textures		Dissimilar Background Biases		Many Objects	
	SR \uparrow	MR \downarrow	SR \uparrow	MR \downarrow	SR \uparrow	MR \downarrow	SR \uparrow	MR \downarrow
SDXL	48.0%	6.5%	58.0%	7.5%	46.0%	22.5%	23.0%	27.5%
+obj	58.0%	5.0%	64.0%	6.5%	51.0%	23.0%	30.0%	29.5%
+EOT/pool	57.0%	4.5%	68.0%	5.0%	59.5%	17.5%	36.5%	16.0%
+obj+EOT/pool	64.0%	3.5%	71.5%	3.5%	68.5%	17.0%	48.0%	15.5%

Table 4: Ablation study on the types of text embeddings modified by DOS. We compare applying DOS to only the semantic token embeddings (obj) or only the EOT/pooled embeddings, against our default approach that modifies all.

Method	Similar Shapes		Similar Textures		Dissimilar Background Biases		Many Objects	
	SR \uparrow	MR \downarrow	SR \uparrow	MR \downarrow	SR \uparrow	MR \downarrow	SR \uparrow	MR \downarrow
SDXL	48.0%	6.5%	58.0%	7.5%	46.0%	22.5%	23.0%	27.5%
Ours ($\alpha = 0.5$)	60.5%	4.5%	67.5%	6.5%	67.0%	19.5%	41.0%	25.5%
Ours (adaptive α 's)	64.0%	3.5%	71.5%	3.5%	68.5%	17.0%	48.0%	15.5%

Table 5: Ablation study comparing adaptive strengths against a fixed strength of $\alpha = 0.5$.

tial performance improvements compared to the baseline. This suggests that the modification directions specified by the separation vectors are effective on its own, even without adaptive strength modulation. However, applying adaptive strength results in even better performance, indicating that modulating the strength of separation differently for each object pair further enhances image generation with multiple objects. An additional ablation study is provided in Table 12 of Appendix C.4, examining sensitivity to predefined words and phrases used to compute adaptive strengths.

6 Limitation

We demonstrated that the adaptive strengths (defined in Eq. 5) in DOS effectively adjust the magnitude of separa-

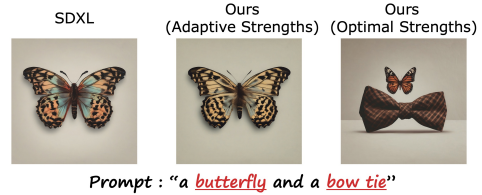


Figure 6: Example where adaptive strengths fail to properly scale separation vectors, leading to object neglect.

tion vectors, leading to improved multi-object image generation (see Table 5). However, as shown in Figure 6, it does not always yield the optimal strengths. In this figure, we compare the default adaptive strength with the optimal strength obtained via grid search over 121 hyperparameter settings (an 11×11 grid with a 0.1 interval). Although such cases are rare, they suggest that there is still room to improve how the strength of each separation vector is determined, potentially by incorporating additional criteria beyond shape, texture, and background bias.

7 Conclusion

In this work, we propose DOS (Directional Object Separation), an efficient and effective method for modifying text embeddings to improve multi-object image generation. Through extensive studies, we identify four problematic scenarios where inter-object relationships frequently cause failures such as object neglect or object mixing. Motivated by two key observations about CLIP embeddings, we construct DOS vectors and add them to three types of CLIP text embeddings before passing them into T2I models. This approach not only offers a practical solution to challenges in multi-object image generation but also demonstrates how the properties of CLIP embeddings can be leveraged to address limitations in downstream models that rely on them.

Acknowledgments

This work was supported by Basic Science Research Program through the National Research Foundation of Korea (NRF) funded by the Ministry of Education (No. RS-2022-NR070876) and in part by Institute of Information & communications Technology Planning & Evaluation (IITP) grant funded by the Korea government (MSIT) ([NO.RS-2021-II211343, Artificial Intelligence Graduate School Program (Seoul National University)], [No.RS-2023-00235293, Development of autonomous driving big data processing, management, search, and sharing interface technology to provide autonomous driving data according to the purpose of usage]).

References

- Black Forest Labs. 2025. Announcing Black Forest Labs.
- Chefer, H.; Alaluf, Y.; Vinker, Y.; Wolf, L.; and Cohen-Or, D. 2023. Attend-and-excite: Attention-based semantic guidance for text-to-image diffusion models. *ACM transactions on Graphics (TOG)*, 42(4): 1–10.
- Chen, C.-Y.; Tseng, C.; Tsao, L.-W.; and Shuai, H.-H. 2024. A cat is a cat (not a dog!): Unraveling information mix-ups in text-to-image encoders through causal analysis and embedding optimization. *Advances in Neural Information Processing Systems*, 37: 57944–57969.
- Google. 2025. Gemini-2.0-Flash-Lite. Version gemini-2.0-flash-lite-001; accessed 10/10/2025.
- Honnibal, M.; Montani, I.; Van Landeghem, S.; and Boyd, A. 2020. spaCy: Industrial-strength Natural Language Processing in Python. *Zenodo*.
- Hu, T.; Li, L.; van de Weijer, J.; Gao, H.; Shahbaz Khan, F.; Yang, J.; Cheng, M.-M.; Wang, K.; and Wang, Y. 2024a. Token merging for training-free semantic binding in text-to-image synthesis. *Advances in Neural Information Processing Systems*, 37: 137646–137672.
- Hu, X.; Wang, R.; Fang, Y.; Fu, B.; Cheng, P.; and Yu, G. 2024b. Ella: Equip diffusion models with llm for enhanced semantic alignment. *arXiv preprint arXiv:2403.05135*.
- Jiang, D.; Song, G.; Wu, X.; Zhang, R.; Shen, D.; Zong, Z.; Liu, Y.; and Li, H. 2024. Comat: Aligning text-to-image diffusion model with image-to-text concept matching. *Advances in Neural Information Processing Systems*, 37: 76177–76209.
- Khalafi, S.; Ding, D.; and Ribeiro, A. 2024. Constrained diffusion models via dual training. *Advances in Neural Information Processing Systems*, 37: 26543–26576.
- Lin, T.-Y.; Maire, M.; Belongie, S.; Hays, J.; Perona, P.; Ramanan, D.; Dollár, P.; and Zitnick, C. L. 2014. Microsoft coco: Common objects in context. In *European conference on computer vision*, 740–755. Springer.
- Liu, S.; Zeng, Z.; Ren, T.; Li, F.; Zhang, H.; Yang, J.; Jiang, Q.; Li, C.; Yang, J.; Su, H.; et al. 2024. Grounding dino: Marrying dino with grounded pre-training for open-set object detection. In *European conference on computer vision*, 38–55. Springer.
- Meral, T. H. S.; Simsar, E.; Tombari, F.; and Yanardag, P. 2024. Conform: Contrast is all you need for high-fidelity text-to-image diffusion models. In *Proceedings of the IEEE/CVF Conference on Computer Vision and Pattern Recognition*, 9005–9014.
- Nguyen, T.; Ilharco, G.; Wortsman, M.; Oh, S.; and Schmidt, L. 2022. Quality not quantity: On the interaction between dataset design and robustness of clip. *Advances in Neural Information Processing Systems*, 35: 21455–21469.
- OpenAI. 2024. GPT-4o-mini: An OpenAI Reasoning Model. Version gpt-4o-mini; accessed 07/16/2025.
- OpenAI. 2025. GPT-o4-mini-high: An OpenAI Reasoning Model. Version gpt-o4-mini-high; accessed 07/16/2025.
- Podell, D.; English, Z.; Lacey, K.; Blattmann, A.; Dockhorn, T.; Müller, J.; Penna, J.; and Rombach, R. 2023. SDXL: Improving Latent Diffusion Models for High-Resolution Image Synthesis. *arXiv preprint arXiv:2307.01952*.
- Qin, Y.; Zheng, H.; Yao, J.; Zhou, M.; and Zhang, Y. 2023. Class-balancing diffusion models. In *Proceedings of the IEEE/CVF Conference on Computer Vision and Pattern Recognition*, 18434–18443.
- Qiu, W.; Wang, J.; and Tang, M. 2025. Self-Cross Diffusion Guidance for Text-to-Image Synthesis of Similar Subjects. In *Proceedings of the Computer Vision and Pattern Recognition Conference*, 23528–23538.
- Radford, A.; Kim, J. W.; Hallacy, C.; Ramesh, A.; Goh, G.; Agarwal, S.; Sastry, G.; Askell, A.; Mishkin, P.; Clark, J.; et al. 2021. Learning transferable visual models from natural language supervision. In *International conference on machine learning*, 8748–8763. PmLR.
- Raffel, C.; Shazeer, N.; Roberts, A.; Lee, K.; Narang, S.; Matena, M.; Zhou, Y.; Li, W.; and Liu, P. J. 2020. Exploring the limits of transfer learning with a unified text-to-text transformer. *Journal of machine learning research*, 21(140): 1–67.
- Rassin, R.; Hirsch, E.; Glickman, D.; Ravfogel, S.; Goldberg, Y.; and Chechik, G. 2023. Linguistic binding in diffusion models: Enhancing attribute correspondence through attention map alignment. *Advances in Neural Information Processing Systems*, 36: 3536–3559.
- Schuhmann, C.; Vencu, R.; Beaumont, R.; Kaczmarczyk, R.; Mullis, C.; Katta, A.; Coombes, T.; Jitsev, J.; and Komatsuzaki, A. 2021. Laion-400m: Open dataset of clip-filtered 400 million image-text pairs. *arXiv preprint arXiv:2111.02114*.
- Stability AI. 2024. Introducing Stable Diffusion 3.5. <https://stability.ai/news/introducing-stable-diffusion-3-5>. Accessed: 07/16/2025.
- Wei, T.; Chen, D.; Zhou, Y.; and Pan, X. 2024. Enhancing mmdit-based text-to-image models for similar subject generation. *arXiv preprint arXiv:2411.18301*.
- Wu, Y.; Yang, X.; and Wang, X. 2024. Relation rectification in diffusion model. In *Proceedings of the IEEE/CVF Conference on Computer Vision and Pattern Recognition*, 7685–7694.

Xu, H.; Xie, S.; Tan, X.; Huang, P.-Y.; Howes, R.; Sharma, V.; Li, S.-W.; Ghosh, G.; Zettlemoyer, L.; and Feichtenhofer, C. 2024. Demystifying CLIP Data. In *The Twelfth International Conference on Learning Representations*.

Zhuang, C.; Hu, Y.; and Gao, P. 2024. Magnet: We never know how text-to-image diffusion models work, until we learn how vision-language models function. *Advances in Neural Information Processing Systems*, 37: 57115–57149.

DOS: Directional Object Separation in Text Embeddings for Multi-Object Image Generation

Supplementary Material

A Details on Preliminary Analysis

In Table 6, we present the prompt templates and object tuples used to construct the prompt sets for each condition in our preliminary analysis (Section 3).

Aspect	Condition	Prompt Template	Object Tuples
Shape	Dissimilar	“a/an {object A} and a/an {object B}”	(coin, brick), (donut, chocolate bar), (plate, ice cube), (basketball, television), (balloon, window), (coin, chocolate bar), (donut, soap bar), (basketball, picture frame), (balloon, monitor), (orange, sugar cube), (shoebox, clock), (soap bar, ring), (sugar cube, frisbee), (monitor, orange), (picture frame, bubble), (brick, ring), (ice cube, frisbee), (television, bubble), (picture frame, orange), (brick, bubble)
	Similar	“a/an {object A} and a/an {object B}”	(coin, clock), (donut, ring), (plate, frisbee), (basketball, orange), (balloon, bubble), (coin, ring), (donut, frisbee), (basketball, bubble), (balloon, orange), (orange, bubble), (shoebox, brick), (soap bar, chocolate bar), (sugar cube, ice cube), (monitor, television), (picture frame, window), (brick, chocolate bar), (ice cube, soap bar), (television, picture frame), (picture frame, monitor), (brick, sugar cube)
Texture	Dissimilar	“a/an {object A} and a/an {object B}”	(fur coat, coin), (peach, saucepan), (sweater, wrench), (cardigan, belt buckle), (rabbit, kettle), (fur coat, key), (mitten, knife), (sweater, saucepan), (puppy, kettle), (cardigan, wrench), (screw, moss patch), (key, mink coat), (bolt, mitten), (ring, towel), (medal, puppy), (screw, peach), (belt buckle, mink coat), (wrench, moss patch), (ring, peach), (saucepan, sweater)
	Similar	“a/an {object A} and a/an {object B}”	(fur coat, moss patch), (peach, mink coat), (sweater, mitten), (cardigan, towel), (rabbit, puppy), (fur coat, peach), (mitten, mink coat), (sweater, towel), (puppy, moss patch), (cardigan, sweater), (screw, coin), (key, saucepan), (bolt, wrench), (ring, belt buckle), (medal, kettle), (screw, key), (belt buckle, saucepan), (wrench, screw), (ring, kettle), (saucepan, wrench)
Background Bias	Similar	“a/an {object A} and a/an {object B}”	(goat, sheep), (monkey, chicken), (lion, deer), (pig, chicken), (cow, monkey), (chicken, lion), (goat, rabbit), (rabbit, gorilla), (chicken, sheep), (monkey, deer), (seahorse, octopus), (shrimp, whale), (dolphin, starfish), (jellyfish, shark), (shark, clownfish), (dolphin, seahorse), (starfish, whale), (seahorse, clownfish), (shrimp, shark), (tuna, shrimp)
	Dissimilar	“a/an {object A} and a/an {object B}”	(goat, octopus), (monkey, whale), (lion, starfish), (pig, shark), (cow, octopus), (chicken, seahorse), (goat, whale), (rabbit, clownfish), (chicken, shark), (monkey, shrimp), (seahorse, sheep), (shrimp, chicken), (dolphin, deer), (jellyfish, chicken), (shark, monkey), (dolphin, lion), (starfish, rabbit), (seahorse, gorilla), (shrimp, sheep), (tuna, deer)
Object Count	Few	“a/an {object A}”	(dog), (cat), (lion), (horse), (penguin), (rabbit), (gorilla), (bear), (cow), (monkey)
		“a/an {object A} and a/an {object B}”	(dog, cat), (cat, lion), (horse, penguin), (rabbit, gorilla), (penguin, horse), (bear, cow), (horse, lion), (rabbit, cat), (cow, penguin), (dog, lion)
	Many	“a/an {object A}, a/an {object B}, and a/an {object C}”	(dog, cat, horse), (cat, lion, penguin), (horse, penguin, cat), (rabbit, gorilla, cow), (penguin, horse, gorilla), (bear, cow, horse), (horse, lion, cat), (rabbit, cat, dog), (cow, penguin, dog), (dog, lion, cat)
		“a/an {object A}, a/an {object B}, a/an {object C}, and a/an {object D}”	(dog, cat, horse, gorilla), (cat, lion, penguin, bear), (horse, penguin, cat, lion), (rabbit, gorilla, cow, cat), (penguin, horse, gorilla, rabbit), (bear, cow, horse, penguin), (horse, lion, cat, penguin), (rabbit, cat, dog, cow), (cow, penguin, dog, gorilla), (dog, lion, cat, rabbit)

Table 6: Prompt templates and object tuples used to construct the prompt sets for each condition in our preliminary analysis (Section 3).

B Experimental Details

B.1 Implementation details

All experiments are conducted on a single NVIDIA RTX 3090 GPU. Our method builds on SDXL (Podell et al. 2023) and is also implemented with the recently released Stable Diffusion 3.5 (SD3.5) (Stability AI 2024). To construct the adaptive strengths defined in Eq. 5, we use 42 representative words covering a diverse range of object shapes and textures and 36 representative background phrases, which are selected through interaction with GPT-o4-mini-high (OpenAI 2025). The full lists of these words and phrases are shown in Table 7. Table 8 presents the offsets used in the shifted tempered sigmoid function in Eq. 5, provided for each base model and embedding type. All offsets are pre-computed over all object pairs from 80 MS-COCO (Lin et al. 2014) classes.

Category	Selected Words or Phrases
Shape or Texture	round, oval, square, rectangular, triangular, spherical, cylindrical, conical, flat, elongated, pointed, curved, ring-shaped, disc-shaped, irregular, spiral, star-shaped, jagged, boxy, stocky, smooth, rough, bumpy, grainy, granular, fuzzy, hairy, woolly, leathery, scaly, feathery, slimy, wrinkled, shaggy, shiny, matte, porous, spongy, striped, spotted, patterned, rubbery
Background	in a forest, in a desert, on a mountain, on a beach, in a grassland, in the Arctic, in the savanna, on the ocean surface, underwater, in a river, in a lake, in a coral reef, in a cave, in a city street, in a suburban neighborhood, in a farm field, at a construction site, at a stadium, in a parking lot, on a road, on a railway track, on a boat deck, on an airport runway, in the sky, in space, in a living room, in a kitchen, in a bedroom, in a bathroom, in an office, in a classroom, in a laboratory, in a factory, in a warehouse, in a shopping mall, in a grocery store

Table 7: Lists of 42 representative words describing object shapes and textures and 36 representative background phrases, used to construct attribute and background prompts for computing adaptive strengths defined in Eq. 5.

Base Model	Offset	Embedding Type (τ)		
		obj	EOT	pool
SDXL	$x_{\tau,0}^{\text{attr}}$	0.5550	0.5474	0.5366
	$x_{\tau,0}^{\text{bg}}$	0.1592	0.3862	0.5835
SD3.5	$x_{\tau,0}^{\text{attr}}$	0.5536	0.5473	0.6168
	$x_{\tau,0}^{\text{bg}}$	0.1705	0.3877	0.4325

Table 8: Offsets $x_{\tau,0}^{\text{attr}}$ and $x_{\tau,0}^{\text{bg}}$ in Eq. 5 for each base model (SDXL, SD3.5) and each embedding type $\tau \in \{\text{obj}, \text{EOT}, \text{pool}\}$.

B.2 Benchmark details

We construct four benchmarks corresponding to the problematic scenarios reported in Figure 1, which are used in our main experiments: Similar Shapes, Similar Textures, and Dissimilar Background Biases, and Many Objects. Each of the first three benchmarks consists of 50 two-object prompts, following the template of “a/an *{object A}* and a/an *{object B}*.” The object pairs for these benchmarks are

selected through interactions with GPT-o4-mini-high (OpenAI 2025). For example, to obtain 50 object pairs for the Similar Shapes benchmark, we ask the model: “Suggest 50 pairs of objects that share a similar overall shape or silhouette, even if they are unrelated in nature.” For the Many Objects benchmark, we extend the animal list used in Attend-and-Excite to include 17 animals, from which we randomly sample to create 25 three-object prompts and 25 four-object prompts. The extended animal list is defined as [cat, dog, bird, bear, lion, horse, elephant, monkey, frog, turtle, rabbit, fish, panda, cow, gorilla, penguin, chicken]. Table 9 shows the prompt templates and object tuples used to construct 50 prompts for each benchmark.

Benchmark	Prompt Template	Object Tuples
Similar Shapes	“a/an {object A} and a/an {object B}”	(basketball, orange), (balloon, ball), (coin, button), (mushroom, umbrella), (soap, eraser), (bicycle, motorcycle), (plate, frisbee), (crayon, candle), (soda can, battery), (golf club, hockey stick), (tent, pyramid), (traffic cone, party hat), (carrot, ice cream cone), (snake, rope), (leaf, feather), (horseshoe, magnet), (soccer ball, globe), (light bulb, onion), (jellyfish, parachute), (butterfly, bow tie), (tennis ball, lime), (hedgehog, hairbrush), (coin, clock), (remote control, chocolate bar), (comb, rake), (jellybean, kidney bean), (matchstick, pencil), (marker, lipstick), (donut, ring), (pebble, almond), (jellyfish, octopus), (penguin, bowling pin), (donut, compact disc), (cabbage, balloon), (pencil, straw), (broom, spear), (screwdriver, paintbrush), (onion, egg), (fork, trident), (shovel, oar), (battery, bullet), (coin, medal), (hourglass, dumbbell), (car tire, lifebuoy), (paperclip, pretzel), (rocket, carrot), (donut, lifebuoy), (clock, wheel), (balloon, bubble), (book, brick)
Similar Textures	“a/an {object A} and a/an {object B}”	(zebra, referee shirt), (leopard, giraffe), (diamond, ice cube), (belt, wallet), (waffle, honeycomb), (coral, sponge), (popcorn, cauliflower), (sandcastle, sugar cube), (loaf of bread, cork), (cactus, pineapple), (marble, ice cube), (sock, mitten), (fur coat, moss patch), (soap, candle), (key, spoon), (strawberry, golf ball), (jellyfish, plastic bag), (kiwi, coconut), (soccer ball, turtle shell), (cactus, sea urchin), (crab, shrimp), (bottle, jar), (fork, spoon), (sheep, cotton ball), (kiwi bird, coconut), (tarantula, carpet), (crocodile, leather handbag), (tiger, clownfish), (panda, soccer ball), (penguin, tuxedo), (giraffe, cheetah), (mirror, chrome ball), (coin, spoon), (carpet, rabbit), (mink coat, peach), (leopard, dalmatian), (teddy bear, peach), (fish, sequined dress), (sponge, pumice stone), (leather shoe, basketball), (cherry, grape), (olive, grape), (wine glass, light bulb), (ladybug, dalmatian), (cheetah, ladybug), (pangolin, artichoke), (lobster, shrimp), (sponge, swiss cheese), (brick, sandpaper), (cat, rabbit)
Dissimilar Background Biases	“a/an {object A} and a/an {object B}”	(beach ball, snowball), (coconut, ice cube), (sandcastle, igloo), (kayak, snowboard), (camel, seahorse), (cow, whale), (goat, octopus), (chicken, fish), (chameleon, seahorse), (horse, seal), (chameleon, penguin), (rabbit, seal), (pineapple, coral), (apple, clam), (coconut, starfish), (lettuce, seaweed), (cauliflower, seahorse), (potato, oyster), (lion, whale), (camel, polar bear), (elephant, shark), (cactus, penguin), (penguin, camel), (fish, bicycle), (crocodile, eagle), (deer, shark), (rabbit, crab), (eagle, seahorse), (igloo, desert tent), (snowman, sandcastle), (ice skate, surfboard), (crocodile, camel), (koala, dolphin), (bear, crab), (cat, jellyfish), (giraffe, seahorse), (sofa, tent), (tractor, sailboat), (boat, car), (cactus, seahorse), (cactus, coral), (strawberry, fish), (parrot, penguin), (tank, canoe), (polar bear, kangaroo), (deer, sea turtle), (monkey, octopus), (carrot, seaweed), (carrot, coral), (dog, dolphin)
Many Objects	“a/an {object A}, a/an {object B}, and a/an {object C}”	(penguin, cat, elephant), (panda, frog, horse), (bear, frog, fish), (lion, fish, chicken), (cat, horse, gorilla), (chicken, bear, rabbit), (gorilla, horse, bird), (cat, fish, turtle), (frog, monkey, fish), (panda, gorilla, bird), (dog, rabbit, lion), (cow, panda, turtle), (chicken, bear, monkey), (rabbit, fish, monkey), (bear, fish, bird), (cow, fish, cat), (fish, bear, cat), (chicken, bird, bear), (chicken, lion, cat), (chicken, bear, penguin), (dog, horse, bird), (monkey, turtle, chicken), (cow, gorilla, bird), (lion, turtle, monkey), (horse, frog, fish)
	“a/an {object A}, a/an {object B}, a/an {object C}, and a/an {object D}”	(bear, horse, turtle, frog), (chicken, cat, bear, lion), (bird, cow, horse, turtle), (turtle, fish, horse, dog), (penguin, cat, cow, gorilla), (fish, horse, gorilla, penguin), (cow, chicken, monkey, turtle), (turtle, horse, cow, gorilla), (bird, cat, fish, cow), (rabbit, turtle, cat, penguin), (bird, cat, dog, elephant), (fish, turtle, chicken, frog), (lion, frog, rabbit, fish), (frog, chicken, rabbit, fish), (chicken, frog, monkey, dog), (chicken, elephant, bird, frog), (cat, panda, horse, bear), (turtle, cat, frog, fish), (cat, cow, horse, monkey), (cow, chicken, turtle, rabbit), (fish, bird, bear, turtle), (cat, lion, rabbit, dog), (bear, cat, penguin, chicken), (panda, fish, chicken, monkey), (panda, lion, frog, chicken)

Table 9: Prompt templates and object tuples for the four benchmarks evaluated in our main experiments.

B.3 Evaluation metrics

We adjust the VLM-based metric from EnMMDiT (Wei et al. 2024) to measure both the success rate (SR) and mixture rate (MR) for each generated image. We provided GPT-4o-mini with the generated image and the text prompt used for image generation, asking it to classify each object in the prompt as (1) fully intact, (2) mixed, or (3) absent. SR is calculated as the ratio of images where all objects are classified as fully intact, and MR is calculated as the ratio of images where one or more objects are classified as mixed. Figure 7 shows examples illustrating our VLM-based evaluation.

VLM Task Description:

Analyze the image and for each of the following objects—*{prompt}*—determine whether it:

1. appears **fully intact** — clearly depicted with correct shape, texture, and all native parts present
2. appears **mixed** — blended or merged in shape, texture, or any feature (e.g., scales, skin pattern, tail, fin) from another object
3. is **absent** — not present at all (neither fully intact nor mixed)

Output Format
Provide exactly N comma-separated tokens in this fixed order:
`[object1_status], [object2_status], ..., [objectN_status]`

where each `[*_status]` must be:
 - the object name itself (e.g. `cat`) **only if** it appears **fully intact**
 - `mixed` if it appears blended or mixed **in any way**
 - `absent` if it does not appear either fully intact or mixed

Do **not** include any additional text or explanations.



Prompt: "a rabbit and a crab"
Answer: "rabbit, crab"
Post-process result: Success



Prompt: "a camel and a polar bear"
Answer: "camel, mixed"
Post-process result: Mixture

Figure 7: Examples illustrating our VLM-based evaluation.

B.4 Human preference study

For the human preferences studies in Section 5.2, we used Amazon Mechanical Turk (MTurk) to collect responses, requiring participants to have over 500 HIT approvals, an approval rate above 98%, and US residency. In each survey, participants were shown five images generated from the same text prompt but using different SDXL-based methods, and asked to select the one that best represents all the objects specified in the prompt. Participants were instructed to avoid images with object neglect or object mixing. Each participant answered 20 questions, along with one additional

dummy question designed to assess attentiveness. The correct answer to the dummy question was provided at the beginning of each survey, and only participants who answered it correctly were included in the valid set. As a result, we collected 580, 640, 640, 560 responses from 29, 32, 32, 28 valid participants for each survey, respectively. Figure 8 shows a screenshot of a question used in our human preference studies.

#7: Select the image that best represents all the objects in the list below. *

Before making your selection, consider the following:

1. Are all listed objects present in the image?
2. Are the objects distinct and not merged or mixed together? (Avoid selecting images where objects appear blended.)
3. If you're not sure, select 'No winner'. Use this option only if necessary.

- [Object List]: deer, shark



Image 1



Image 2



Image 3



Image 4



Image 5

No winner. (Try to avoid this option)

Figure 8: A screenshot of a question used in our human preference studies.

C Additional Experiments

C.1 Combining DOS with Attend-and-Excite

Since DOS only modifies CLIP text embeddings, it can be used in combination with other latent modification methods such as Attend-and-Excite (A&E) (Chefer et al. 2023). This combined method addresses some issues that cannot be solved by using either DOS or A&E alone, as shown in Figure 9. We further validate the effectiveness of this combination through a quantitative comparison, presented in Table 10.



Figure 9: Our method, DOS, can be used in combination with other latent modification method such as A&E (Chefer et al. 2023). All methods are based on SDXL.

Method	Similar Shapes		Similar Textures		Dissimilar Background Biases		Many Objects	
	SR \uparrow	MR \downarrow	SR \uparrow	MR \downarrow	SR \uparrow	MR \downarrow	SR \uparrow	MR \downarrow
SDXL	48.0%	6.5%	58.0%	7.5%	46.0%	22.5%	23.0%	27.5%
Ours	64.0%	3.5%	71.5%	3.5%	68.5%	17.0%	48.0%	15.5%
A&E	60.5%	6.0%	67.5%	5.0%	53.5%	25.0%	28.5%	28.5%
A&E+Ours	66.0%	3.0%	73.5%	3.0%	69.0%	14.5%	52.5%	15.0%

Table 10: The combination of DOS and A&E (A&E+Ours) demonstrates a synergistic effect, achieving the best performance across all benchmarks.

C.2 Qualitative ablation on text embedding types

Figure 10 presents qualitative examples from the ablation study on the types of text embeddings to which DOS is applied. Applying DOS only to semantic token embeddings (+obj) or only to EOT/pooled embeddings (+EOT/pool) yields suboptimal results, often exhibiting object neglect or mixing. In contrast, applying DOS to all types of text embeddings produces the best outcomes, clearly representing both objects in the prompt without object mixing.

C.3 Extended Many Objects benchmark

To address concerns regarding the benchmark’s scope and to validate the external validity of our method, we construct an extended Many Objects benchmark with greater categorical diversity. Moving beyond the original animal-only set, we incorporate objects from electronics, vehicles, and fruits. The expanded object list now consists of 16 distinct objects: [cat, dog, frog, fish, smartphone, laptop, television, camera, car, bicycle, motorcycle, train, apple, orange, avocado,

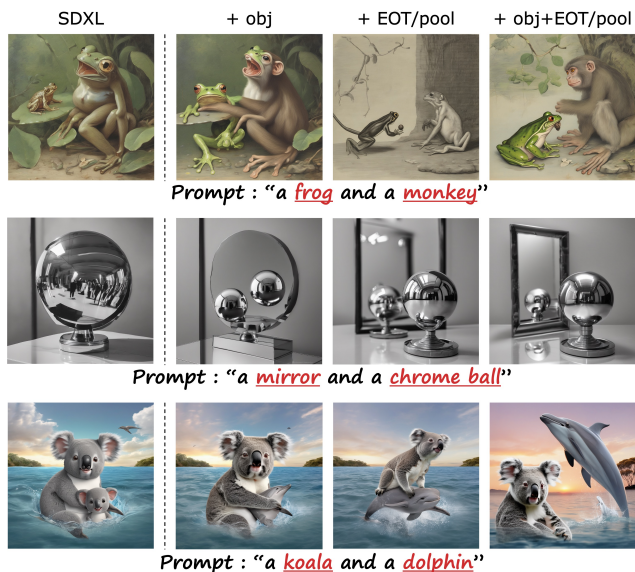


Figure 10: Qualitative results from the ablation study on the types of text embeddings to which DOS is applied. Applying DOS to all types of text embeddings produces the best outcomes, clearly representing both objects in the prompt without object mixing.

strawberry]. From this set, we randomly generate 25 three-object and 25 four-object prompts. As shown in Table 11, the performance trends are consistent with those on the original benchmark presented in Table 1. This result indicates that our method’s effectiveness is not limited to a single category but generalizes across diverse object categories.

Base Model	Method	SR \uparrow	MR \downarrow
SDXL	Base	31.50%	19.50%
	TEBOpt	33.50%	21.50%
	A&E	42.50%	18.50%
	CONFORM	43.50%	21.00%
	Ours	45.00%	14.50%
SD3.5	Base	78.00%	13.00%
	Ours	85.50%	6.00%

Table 11: Performance comparison on the extended Many Objects benchmark. SR denotes Success Rate (\uparrow higher is better), and MR denotes Mixture Rate (\downarrow lower is better). The best results are highlighted in bold.

C.4 Sensitivity to predefined words and phrases

Our adaptive strength utilizes predefined lists of 42 shape/-texture words and 36 background phrases. To ensure our approach is not over-tuned to this specific set, we performed a sensitivity analysis. We created a reduced set by randomly sampling half of these lists (21 words and 18 phrases). We then evaluated the performance of DOS on this reduced set, repeating the process four times and averaging the outcomes. The results, shown in Table 12, reveal that while

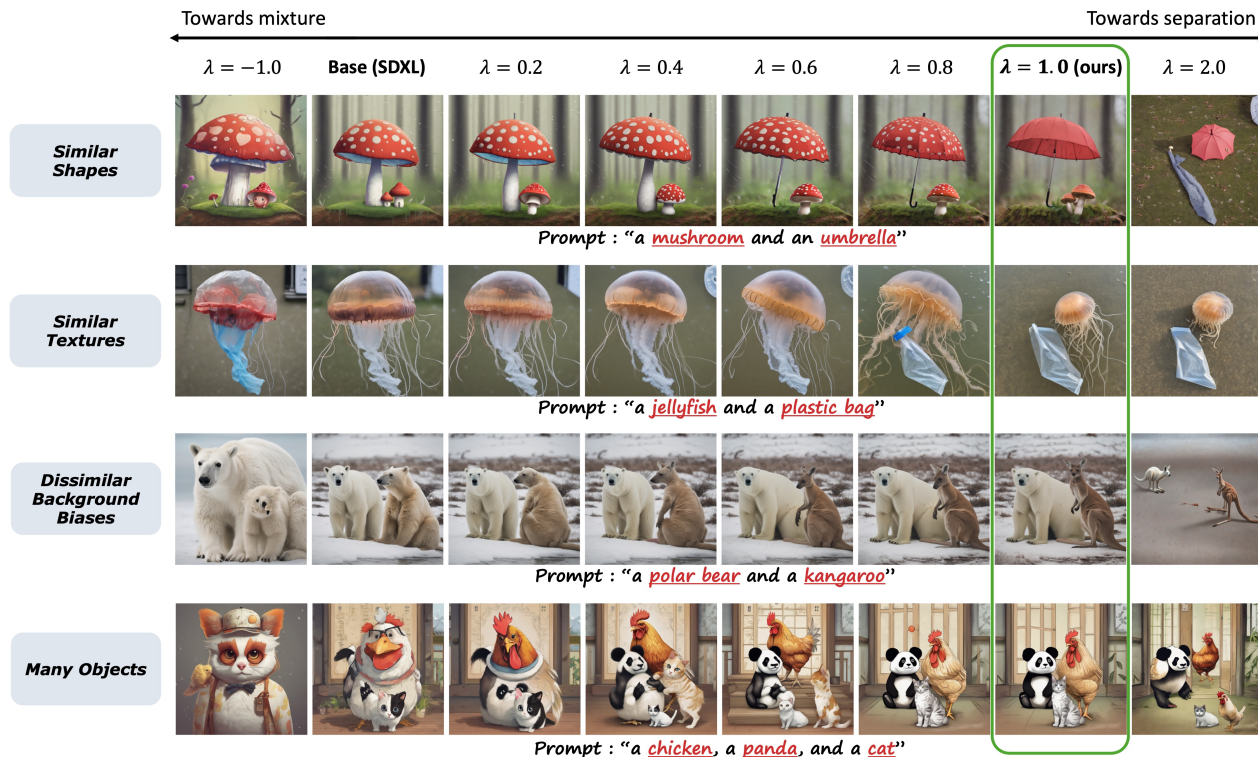


Figure 11: Directional information encoded in DOS vectors. Effect of scaling the directional scaler λ defined in Equations 11-12. As λ increases positively, objects become more separated, while the negative value of λ intensifies object mixing. Excessively large positive values (i.e., $\lambda = 2$) can cause unexpected results due to strong deviation from the original text embeddings. The baseline SDXL corresponds to using $\lambda = 0$, while our default method corresponds to using $\lambda = 1$.

Method	Similar Shapes		Similar Textures		Dissimilar Background Biases		Many Objects	
	SR \uparrow	MR \downarrow	SR \uparrow	MR \downarrow	SR \uparrow	MR \downarrow	SR \uparrow	MR \downarrow
SDXL	48.0%	6.5%	58.0%	7.5%	46.0%	22.5%	23.0%	27.5%
Ours (50% words/phrases)	62.4%	2.4%	69.4%	4.8%	67.4%	18.8%	47.8%	13.9%
Ours (100% words/phrases)	64.0%	3.5%	71.5%	3.5%	68.5%	17.0%	48.0%	15.5%

Table 12: Ablation study on the predefined words and phrases. Performance is compared between using the full list of predefined words and phrases (100%) and a randomly sampled half (50%).

there is a slight drop in performance, the method’s effectiveness is largely maintained. This demonstrates the robustness of our adaptive mechanism, alleviating concerns about its dependency on a fixed, hand-crafted set of priors.

C.5 DOS vectors encode directional information

DOS vectors are weighted sum of separation vectors, where each separation vector reflects the directional information for separating the corresponding object pair. Therefore, DOS vectors may also carry directional information, which can be observed in the generated images. To investigate this, we varied the directional scale of each DOS vector before adding

them to the original CLIP text embeddings as follows:

$$\mathbf{c}_{\text{obj}}^n{}' = \mathbf{c}_{\text{obj}}^n + \lambda \mathbf{v}_{\text{obj}}^{\text{DOS},n}, \quad (11)$$

$$\mathbf{c}'_{\text{EOT}/\text{pool}} = \mathbf{c}_{\text{EOT}/\text{pool}} + \lambda \sum_{i=1}^N \mathbf{v}_{\text{EOT}/\text{pool}}^{\text{DOS},i}, \quad (12)$$

where $n \in 1, \dots, N$ denotes the index of an object, and λ is a directional scaler (which can also take negative values) (Please compare these with Equations 9–10). Figure 11 shows generated images with λ varying from -1.0 to 2.0 for four prompts. As λ increases in the positive direction, the objects in the prompts gradually become more separated. In contrast, when λ is negative, the objects tend to mix more. Lastly, increasing λ too much in the positive direction (e.g., $\lambda = 2$) occasionally leads to unexpected results, possibly due to a strong deviation from the original text embeddings.

C.6 Validation with multiple evaluators

While the Success Rate (SR) and Mixture Rate (MR) in Table 1 were measured using GPT-4o-mini (OpenAI 2024), relying on a single Vision Language Model (VLM) could introduce evaluation biases. To validate the reliability of our evaluation results, we re-evaluated all methods using two additional evaluators: another VLM, Gemini-2.0-Flash-Lite (Google 2025), and an open-vocabulary object detector,

Base Model	Method	Similar Shapes			Similar Textures			Dissimilar Background Biases			Many Objects		
		SR↑ (gemini)	MR↓ (gemini)	SR↑ (g-dino)	SR↑ (gemini)	MR↓ (gemini)	SR↑ (g-dino)	SR↑ (gemini)	MR↓ (gemini)	SR↑ (g-dino)	SR↑ (gemini)	MR↓ (gemini)	SR↑ (g-dino)
SDXL	Base	45.50%	16.00%	24.00%	58.00%	13.50%	39.50%	48.00%	26.50%	43.00%	21.50%	33.00%	17.50%
	TEBOpt	48.50%	20.50%	24.50%	59.00%	11.00%	37.50%	46.00%	27.00%	40.50%	22.00%	36.00%	22.00%
	A&E	50.50%	14.50%	29.50%	65.50%	9.00%	45.50%	62.00%	21.00%	46.00%	33.50%	34.50%	22.50%
	CONFORM	47.50%	14.00%	24.50%	67.00%	10.50%	44.00%	54.00%	23.50%	47.00%	32.50%	31.00%	27.00%
	Ours	54.00%	12.50%	32.50%	68.00%	8.00%	53.50%	69.00%	19.50%	61.50%	46.50%	15.00%	43.50%
SD3.5	Base	73.00%	7.00%	38.00%	84.50%	10.00%	64.50%	88.50%	10.50%	72.50%	67.00%	20.00%	59.50%
	Ours	78.00%	6.00%	44.50%	87.50%	7.00%	70.00%	92.00%	7.50%	75.50%	75.50%	12.00%	70.00%

Table 13: Quantitative comparison using multiple evaluators. We report SR↑ (gemini), MR↓ (gemini), and SR↑ (g-dino) across all four benchmarks. The best results are highlighted in bold.

Method	Similar Shapes		Similar Textures		Dissimilar Background Biases		Many Objects	
	SR↑	MR↓	SR↑	MR↓	SR↑	MR↓	SR↑	MR↓
SD3.5	75.5%	4.0%	79.0%	6.0%	78.0%	17.5%	70.0%	16.5%
TEBOpt	77.5%	3.0%	78.0%	8.0%	81.0%	16.5%	73.0%	14.5%
Self-Cross	77.0%	2.5%	81.0%	8.0%	82.5%	13.5%	71.5%	12.0%
Ours	81.0%	3.0%	87.5%	3.0%	85.5%	13.5%	76.5%	10.5%

Table 14: Performance comparison on SD3.5 as the base model.

Grounding-DINO (Liu et al. 2024). The MR metric was excluded for the object detector as it is not capable of assessing object mixing. The re-evaluated quantitative comparison, presented in Table 13, shows a consistent trend with our main results, suggesting their validity.

C.7 Performance comparison on SD3.5

Our main comparison in Table 1 was conducted on SDXL as the base model. To verify that this performance advantage extends to more recent architectures, we compared our method against TEBOpt (Chen et al. 2024) and Self-Cross (Qiu, Wang, and Tang 2025) using SD3.5 as the base model. Table 14 shows that our approach maintains its superior performance on this newer architecture.

C.8 Additional qualitative comparisons

Qualitative results on A&E benchmark. Although our main benchmarks focus on failures arising from inter-object relationships in *attribute-free* prompts, we additionally demonstrate that DOS maintains and can even improve attribute binding on the widely used Attend-and-Excite (A&E) benchmark (Chefer et al. 2023). The benchmark defines three prompt templates: (i) “a {*animal A*} and a {*animal B*}”, (ii) “a {*animal*} and a {*color*} {*object*}”, and (iii) “a {*color A*} {*object A*} and a {*color B*} {*object B*}”, of which template (iii) is the most challenging because the model must correctly bind two independent color-object pairs in a single image. Figures 12 and 13 compare DOS with four baselines on template (iii): SDXL,

TEBOpt, A&E, and CONFORM. Despite the absence of an explicit attribute-object binding guidance, DOS consistently keeps each color attached to the correct object and delivers clearer separation between the two objects, whereas competing methods often fail to bind attributes correctly or neglect the objects. Although the separation vectors in DOS were devised to mitigate inter-object interference, they also implicitly preserve the binding between attributes and objects. These results suggest that DOS can be applied effectively to general prompts containing multiple attribute-object tuples, extending its utility beyond specific scenarios.

Additional qualitative results. Figures 14–16 present additional qualitative results on the four benchmarks, and Figure 17 presents additional qualitative results on complex prompts.



Figure 12: Qualitative comparison on A&E benchmark (Part 1 of 2).

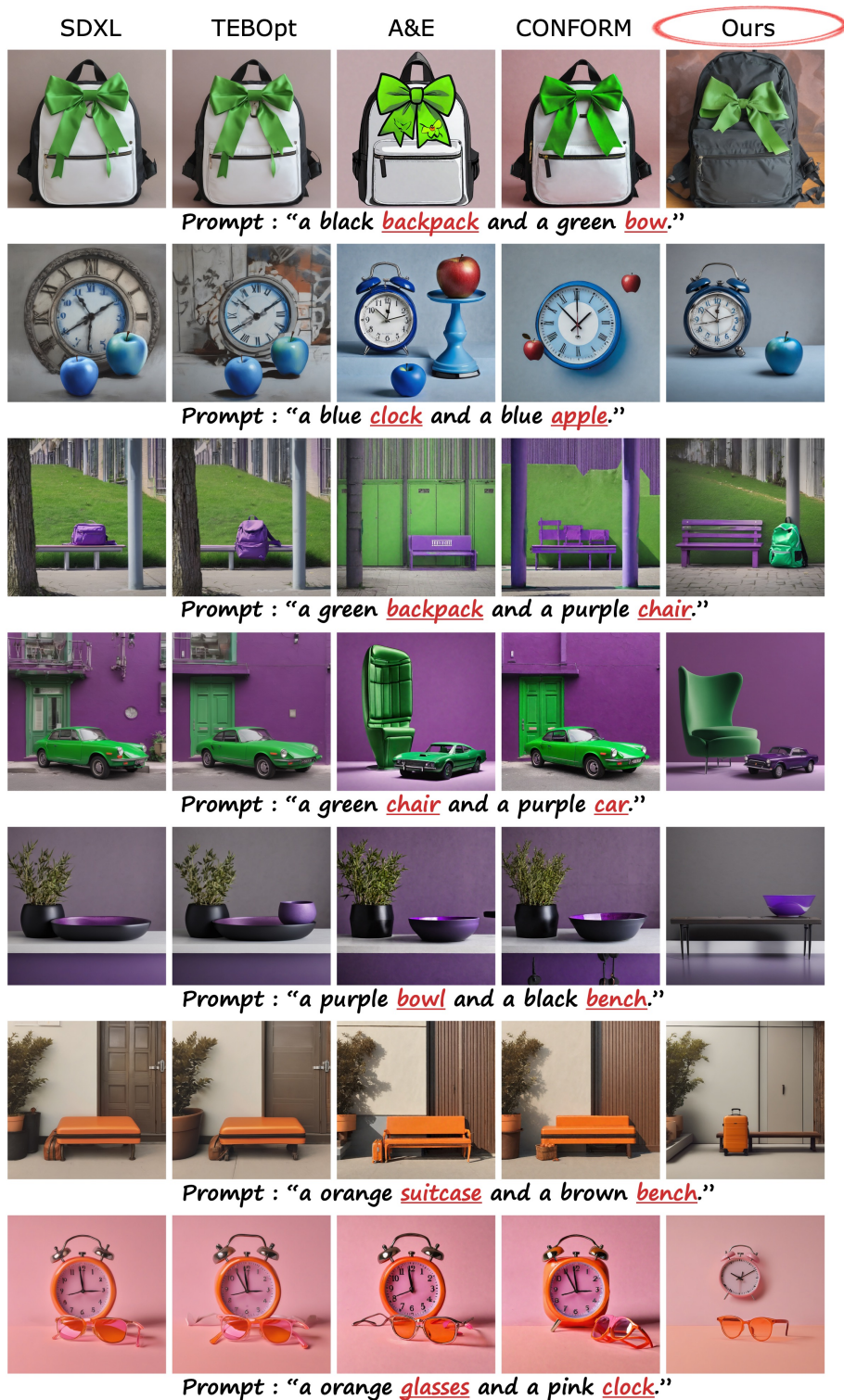


Figure 13: Qualitative comparison on A&E benchmark (Part 2 of 2).



Figure 14: Additional qualitative results on our four benchmarks (Part 1 of 3).

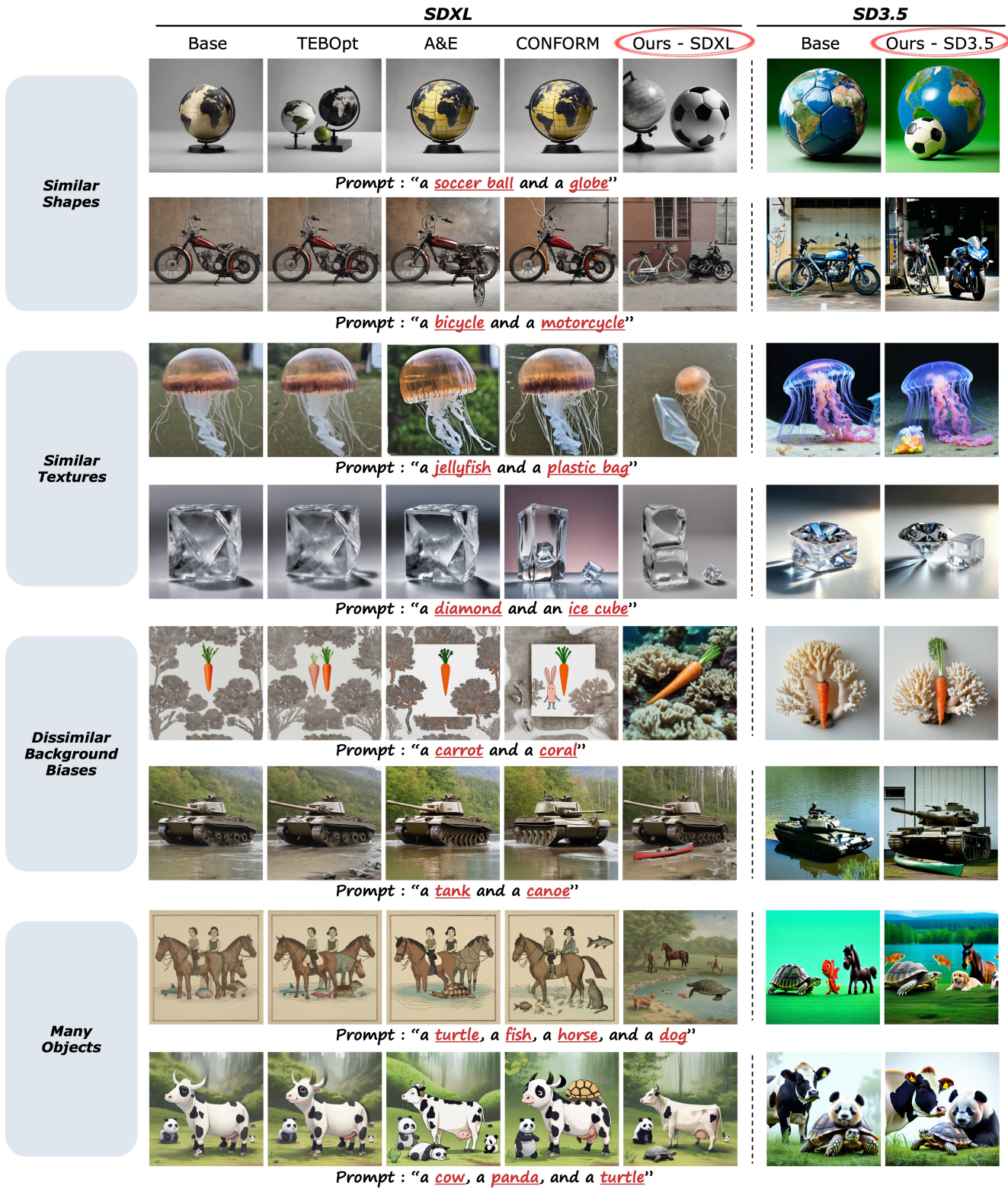


Figure 15: Additional qualitative results on our four benchmarks (Part 2 of 3).

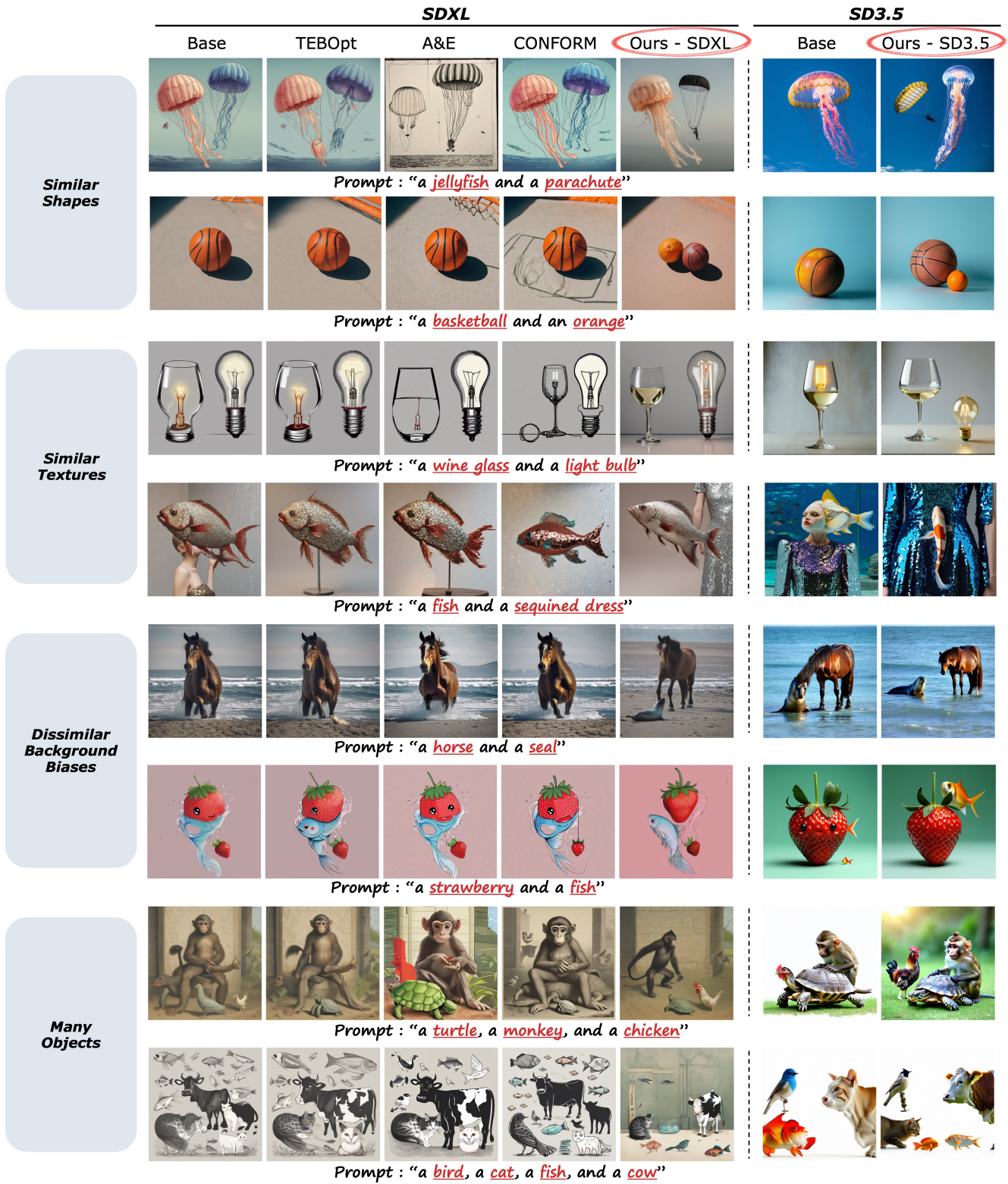


Figure 16: Additional qualitative results on our four benchmarks (Part 3 of 3).

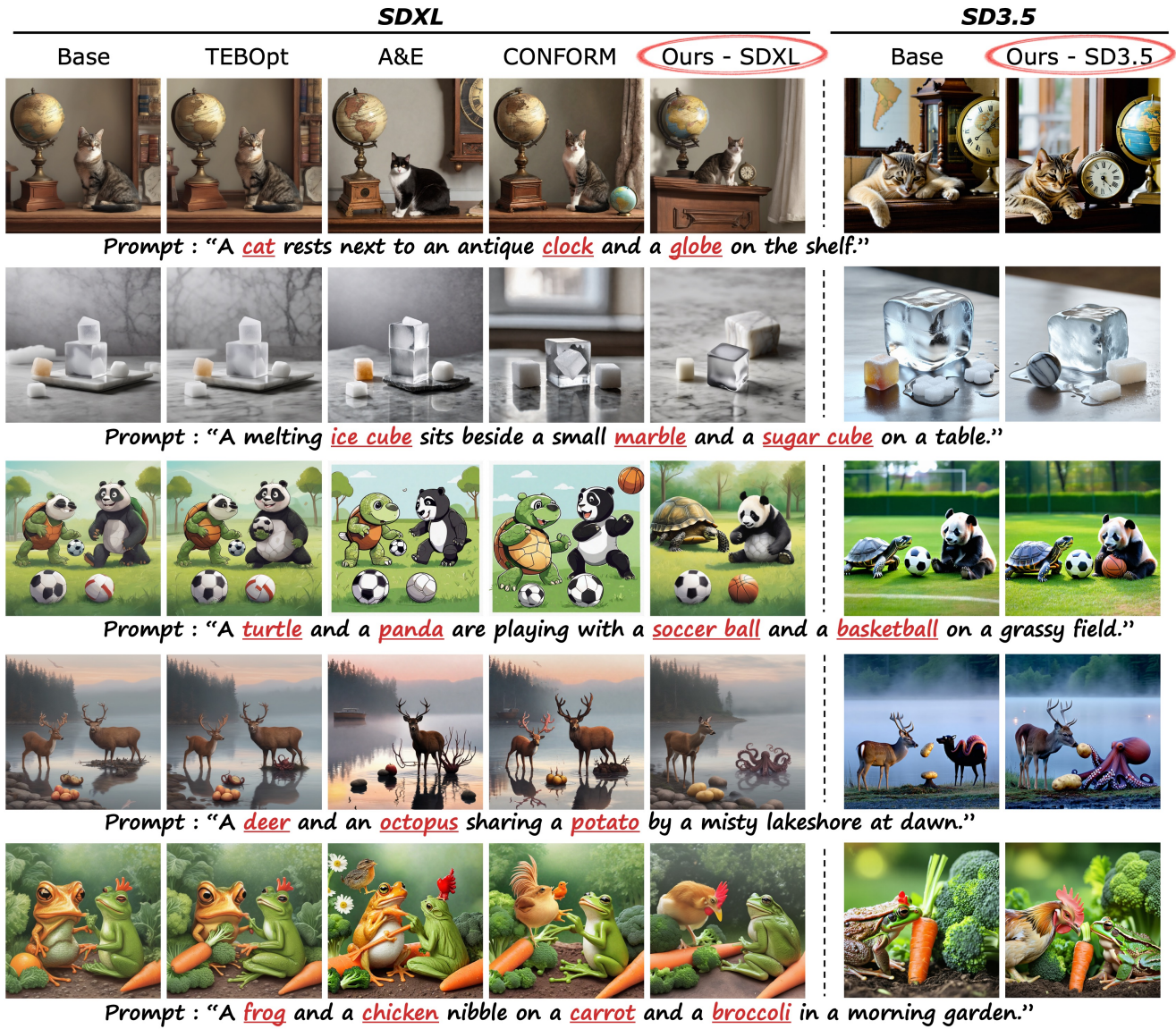


Figure 17: Additional qualitative results on complex prompts.

D Directional Encoding Across CLIP Text Embedding Types

One of key motivations for our method is the observation that the difference between two CLIP text embeddings encodes directional information, such as “*king* – *man* + *woman* \approx *queen*” (Hu et al. 2024a). However, prior work has only validated this directional encoding when semantic token and EOT embeddings are used *together*. Since DOS calculates separation vectors *independently* for different embedding types—the semantic token for each object noun and the EOT/pooled embedding—here we test whether this directional property holds for each type of embedding individually.

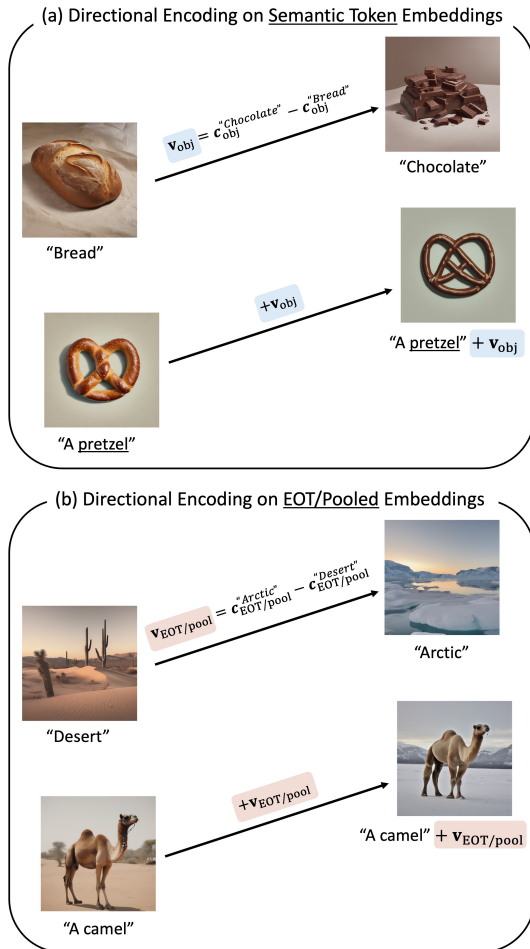


Figure 18: Directional information encoded in the difference between two CLIP text embeddings. (a) *Semantic token embeddings*. The difference between “Chocolate” and “Bread” token embeddings, v_{obj} , is added to the “pretzel” token embedding, turning a bread-like pretzel into a chocolate-coated pretzel. (b) *EOT/pooled embeddings*. The “Arctic–Desert” direction obtained from EOT/pooled embeddings, $v_{\text{EOT/pool}}$, is added to the EOT/pooled embeddings of the prompt “A camel”, converting the desert background into an arctic scene while maintaining the subject.

Let P denote a prompt containing only a single object noun (e.g., “Bread”), and denote the semantic token embedding of this object noun by $c_{\text{obj}}^P \in \mathbb{R}^d$. Given two prompts P_1 and P_2 , each containing a different object, we define a directional vector $v_{\text{obj}} = c_{\text{obj}}^{P_2} - c_{\text{obj}}^{P_1}$. Adding v_{obj} to the semantic token embedding of a third prompt P_3 moves the generated image along the intended direction: the attribute associated with P_1 ’s object fades, whereas that of P_2 ’s object emerges. Figure 18(a) illustrates this behavior—adding the “chocolate–bread” vector to the “pretzel” token embedding replaces bread-like appearance with chocolate-like appearance.

An analogous experiment on the EOT/pooled embeddings is performed by constructing $v_{\text{EOT/pool}} = c_{\text{EOT/pool}}^{\text{Arctic}} - c_{\text{EOT/pool}}^{\text{Desert}}$ and adding it to $c_{\text{EOT/pool}}^{\text{A camel}}$. As shown in Figure 18(b), the background transitions from a desert to an arctic landscape while preserving the foreground camel.

Taken together, these results demonstrate that the directional information captured by the difference between two CLIP text embeddings can be observed independently in both the semantic token embeddings and the EOT/pooled embeddings.

E Training Data Biases Underlying Generation Failures

The representation of the trained models are known to be significantly influenced by the distribution of their training dataset (Nguyen et al. 2022; Qin et al. 2023; Xu et al. 2024; Khalafi, Ding, and Ribeiro 2024). Frequent failures in the two problematic scenarios, Dissimilar Background Biases and Many Objects, can be partially explained by this effect. To investigate this, we analyze all captions in LAION 400M (Schuhmann et al. 2021), a dataset whose filtered subset is believed to be used in training T2I models. Specifically, we compare (i) the co-occurrence rate of object pairs with similar vs. dissimilar background biases, and (ii) the proportion of captions containing varying numbers of noun chunks.

Condition	Object Pair	Intersection / Union	Co-occurrence (%)
Similar Background Biases	camel, ostrich	20 / 40655	0.049
	giraffe, elephant	1228 / 95385	1.287
	shark, whale	1660 / 64800	2.562
	koala, kangaroo	152 / 15641	0.972
	hippo, crocodile	76 / 26204	0.290
	goat, sheep	1026 / 85127	1.205
	crab, octopus	348 / 38095	0.914
	lion, tiger	1185 / 140775	0.842
	penguin, polar bear	307 / 44326	0.693
	eagle, hawk	671 / 60597	1.107
<i>Average</i>			0.992
Dissimilar Background Biases	camel, penguin	13 / 65264	0.020
	shark, elephant	59 / 110663	0.053
	horse, whale	71 / 190411	0.037
	koala, walrus	0 / 9243	0.000
	eagle, crocodile	8 / 69615	0.011
	goat, octopus	3 / 43116	0.007
	giraffe, dolphin	11 / 37966	0.029
	llama, hawk	0 / 17157	0.000
	gorilla, polar bear	3 / 25229	0.012
	kangaroo, jellyfish	9 / 13509	0.067
<i>Average</i>			0.024

Table 15: Co-occurrence rates of object pairs with similar vs. dissimilar background biases in LAION 400M. The co-occurrence rate is computed using the Jaccard index between two objects, calculated as the number of captions containing both objects divided by the number containing at least one. Object pairs with dissimilar background biases co-occur significantly less often than those with similar biases.

In Table 15, we report the co-occurrence rates for two sets of object pairs: one with similar background biases, and the other with dissimilar biases. The co-occurrence rate is defined using the Jaccard index, calculated as the number of captions containing both objects divided by the number of captions containing at least one of them. The results show that object pairs with dissimilar background biases co-occur significantly less frequently than those with similar biases. In Table 16, we examine how the number of noun chunks varies across prompts. Using spaCy (Honnibal et al. 2020) to count noun chunks per caption, we find that over 63% of captions contain fewer than three noun chunks. Together,

these findings provide evidence that the failures of T2I models in these two scenarios are, at least in part, attributable to biases in the training data distribution.

Num. of Noun Chunks	0	1	2	3	4	5	$N > 5$	Total
Percentage (%)	1.18	34.51	28.58	17.29	8.48	4.04	5.92	100

Table 16: Distribution of noun chunk counts in LAION 400M captions. The proportion of captions with varying numbers of noun chunks, extracted using spaCy (Honnibal et al. 2020), shows that over 63% of captions contain fewer than three noun chunks, suggesting limited multi-object descriptions in the training data.